北海道大学工学部研究報告
第136号（昭和62年）

Bulletin of the Faculty of Engineering,
Hokkaido University. No. 136 (1987)

THE INFLUENCE OF PREPARATION CONDITIONS OF POWDER MIXTURES ON THE REACTION OF V_2O_5-Fe_2O_3 SYSTEM

Akira SHIMIZU, Ryusaburo FURUICHI and Tadao ISHII
(Received March 31, 1987)

Abstract

In order to investigate the influence of preparation conditions of powder mixtures on the rate of $FeVO_4$ formation, five mixtures (**M1**-**M5**) were prepared by using three V_2O_5 **V1**, **V2** and **V3**) and two Fe_2O_3 (**F1** and **F2**) powders. **V1** was prepared by thermal decomposition of NH_4VO_3 at 450℃ and **V2**, **V3** were prepared from **V1** by manual grinding in a mortar (**V2**) and by jet mill grinding (**V3**), respectively. **F1** and **F2** were prepared from commercial α-Fe_2O_3 by sieving under 325 mesh (**F1**) and by manual grinding in a mortar (**F2**), respectively. Equimolar mixtures of these V_2O_5 and Fe_2O_3 were obtained by mixing in an agate mortar for 1 hr with a weak force (**w**) and strong force (**s**) respectively. The preparation conditions of the mixtures are as follows: **M1** (**V1**, **F2**, **w**), **M2** (**V2**, **F2**, **w**), **M3** (**V3**, **F2**, **w**), **M4** (**V2**, **F1**, **w**) and **M5** (**V2**, **F2**, **s**). The rate was evaluated by using Jander's equation ($[1-(1-\alpha)^{1/3}]^2=k_jt$). The order of the rate was $k_{jM5} \simeq k_{jM3} > k_{jM2} > k_{jM4} > k_{jM1}$. Particle sizes ($d$) of V_2O_5 and Fe_2O_3 in the mixtures were $d_{V1} > d_{F1} > d_{V2} = d_{V3} = d_{F2}$. Lattice strain ($\eta_a$) of V_2O_5 was estimated by Hall's plot of (200), (400) and (600) planes. The order of η_a-value of V_2O_5 in the mixtures was found to be $\eta_{aM3} > \eta_{aM5} > \eta_{aM2} = \eta_{aM4} > \eta_{aM1}$. The increase in k_j-value was explained by the increase in η_a of V_2O_5 and in the contact point between reacting particles.

1. Introduction

In the reaction of powdery solids, the mixing of the sample powders is a very important process. The differences in mixing conditions, such as mixing technique, force, time and atmospheres will result in mechanochemical effects, such as the changes in particle size, defects, lattice strain and crystallinity. These effects will produce great difficulties in the investigation of the reactivity of powdery solids with different preparation histories[1,2] and in obtaining reproducible data of the reaction. In the present paper the rate of $FeVO_4$ formation was studied by using five mixtures of V_2O_5-Fe_2O_3, which were prepared by mortar mixing under different mixing conditions. The results were discussed on the basis of the changes in particle size and lattice strain of V_2O_5 powders arising in the mixing process.

Department of Applied Chemistry, Faculty of Engineering Hokkaido University

2. Experimental

2. 1 Material

Three V_2O_5 samples (**V1**, **V2** and **V3**) and two Fe_2O_3 samples (**F1** and **F2**) were prepared as follows;

V1: decomposition of NH_4VO_3 (2 g, −250 mesh) at 450℃ for 1 hr in an air stream of 100 m*l*/min[1].

V2: grinding of **V1** in an agate mortar using a pestle with a strong force and sieving to allow for passing through 325 mesh sive.

V3: grinding of **V1** by jet mill (Seishin Kigyo Co. Ltd.) for 20 min.

F1: sieving of commercial α-Fe_2O_3 to pass through 325 mesh sieve.

F2: grinding of commercial α-Fe_2O_3 (100-150 mesh) in an agate mortar by pestle with a strong force and sieving to pass through 325 mesh sieve.

X-ray diffraction patterns of these V_2O_5 and Fe_2O_3 agreed with ASTM cards 9-387 and 13-534.

2. 2 Mixing methods

The mixing was carried out in an agate mortar for 1 hr. The mixing ratio of V_2O_5 to Fe_2O_3 was 1:1 in mole (V_2O_5=2.183 g, Fe_2O_3=1.916 g). Five mixtures (**M1**-**M5**) were prepared by applying a weak force and or a strong force;

M1: **V1** and **F2** with weak mixing force.

M2: **V2** and **F2** with weak mixing force.

M3: **V3** and **F2** with weak mixing force.

M4: **V2** and **F1** with weak mixing force.

M5: **V2** and **F2** with strong mixing force.

X-ray diffraction patterns of these five mixtures showed a mixed phase of V_2O_5 and Fe_2O_3. The completeness of the mixing was tested by chemical analysis of V_2O_5 content in several portions (200 mg) of the mixtures. The content was within an experimental error of ±2%. The method of chemical analysis of V_2O_5 is described in section **2. 4.**

2. 3 Reaction method

The reaction was carried out at temperataures of 525-625℃ in static air. The sample mixture of 600 mg was packed in an alumina boat (7×15 mm) and placed in a horizontal electric furnace. The reaction time measurement was started just after the sample was placed in the furnace kept at a fixed temperature.

2. 4 Measurement of conversion

Fractional conversion (α) of $FeVO_4$ was estimated from the amount of V_2O_5 remaining in the mixture after the reaction. A sample of 200 mg was dissolved in 200 ml of 1.5M-H_2SO_4 for 10 min at room temperature. The amount of V^{5+} in acid was measured with potentiometric titration using 1/60M-Mohr's salt solution. Titraion error was within ±2%. The dissolution time of 10 min was found to be suitable from two facts in which pure V_2O_5 and the mixture before the reaction were completely dissolved in 1.5M-H_2SO_4 within 10 min

and that the solubility of $FeVO_4$ (prepared from **M5** after reaction at 650℃ for 24 hr) was only 2% under the same condition which is within the titration error. These facts suggest that the dissoluion rate of $FeVO_4$ is negligible compared with that of unreacted V_2O_5 in the mixtures. The reproducibility of α-value was estimated to be ±2% from **M1**, **M2** and **M3** reacted at 600℃ for 3 hr.

2. 5 SEM photograph

SEM photograph of the sample was taken by using an apparatus MSM-4 manufacturedly Hitachi-Akashi Co. Ltd.. The sample was dispersed in ethanol by ultrasonic wave generator and then sedimented in the sample holder (alumina disk, $\phi = 15$ mm). The sample was coated with gold in a vacuum evaporator (Eiko Co. Ltd. IB-3) to avoid the electrification.

2. 6 X-ray diffraction

X-ray diffaction (Geigerflex 2142 Rigakudenki Co. Ltd.) was used to identify the samples before and after the reaction and to measure the diffraction angle (2θ) and the peak breadth at half-maximum intensity (β_{hkl}) of V_2O_5, Fe_2O_3 and $FeVO_4$. The peak profile for the determination of 2θ and β_{hkl}-values was obtained by manual step scan method. The scan was carried out by moving the goniometer every 1/100 degrees. The intensities were measured five times at each diffraction angle for 10 sec. Cu, Co and Cr-targets were used for the measurments of 2θ and β_{hkl}-values. The β_{hkl}-value was determined by Bartram's method[3]. A standrd V_2O_5 samples was prepared by calcining **V2** at 600℃ for 10 hr in air. This V_2O_5 was found to consist of single crystal grains of 0.2-1.7 μm in size with hardly any strain which showed a regular spot pattern of electron diffraction. However, single crystal grains of Fe_2O_3 and $FeVO_4$ could not be prepared, thus silicon powder obtained by grinding silicon lamp (Wakojunyaku Co. Ltd.) was used as the standard sample.

2. 7 BET surface area

Specific surface areas of V_2O_5 and Fe_2O_3 samples were estimated by BET method. The amount of Ar adsorbed was measured at −195℃ after degassing 0.4 g sample at 10^{-4}mmHg for 10 hr at room terperature.

2. 8 IR measurement

The stretching vibration band of V=O group was measured by KBr disk method, using IR specrometer (Hitachi Seisakusho Co. Ltd. 260-50). The disk was prepared by pressing the mixture of 0.1 mg of sample and 200 mg of KBr powder at a pressure of 5.3 ton/cm^2.

3. Result and discussion

3. 1 The rate of $FeVO_4$ formation

Figure 1 shows the fractional conversion (α) vs. reaction time (t) curves for five mixtures. From X-ray diffraction patterns, $FeVO_4$ was found to be the only product of the reaction. The data in Fig. 1 were examined by the reduced time method[4] using seven kinetic equations. The data fitted Jander's equation[5] (Equation (1)) best.

$$[1-(1-\alpha)^{1/3}]^2 = k_j t \qquad (1)$$

Therefore, V_2O_5-Fe_2O_3 powder reaction is considered to be controlled by the diffusion of

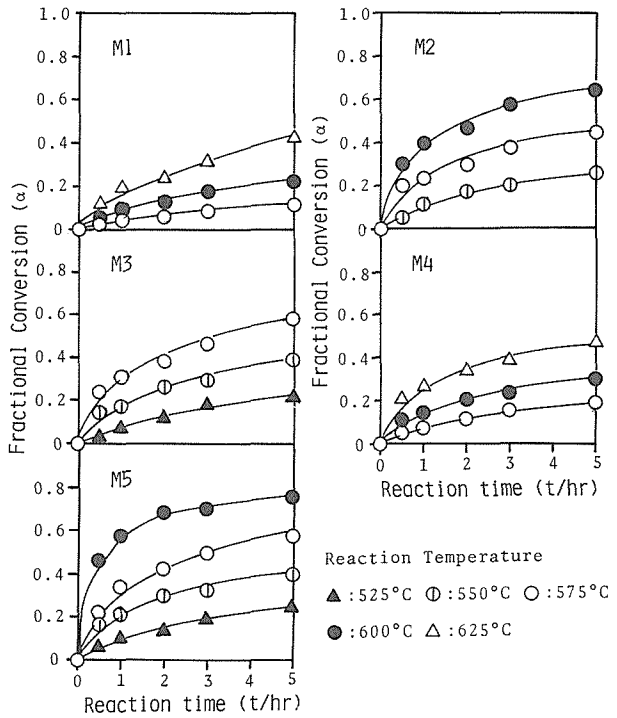

Fig. 1 Fractional conversion (α) vs. reaction time (t) curves of $FeVO_4$ formation for five mixtures.

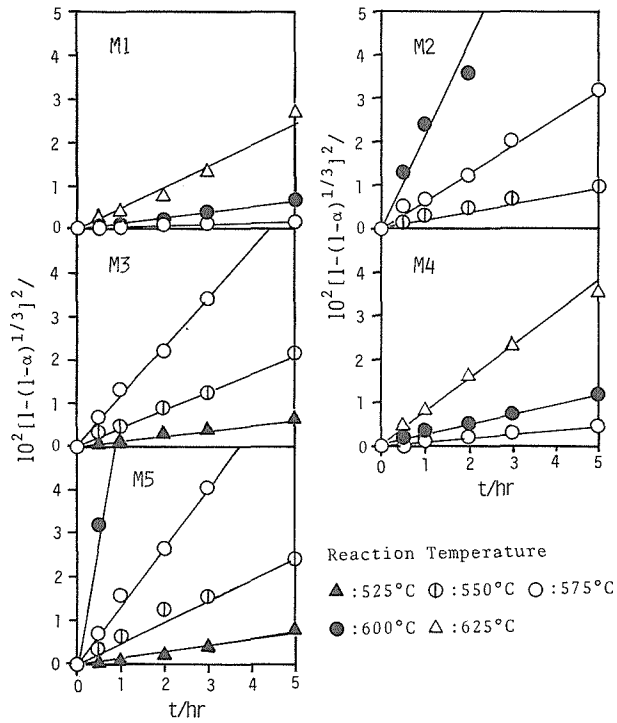

Fig. 2 Plots of $[1-(1-\alpha)^{1/3}]^2$ vs. t at various temperatures for five mixtures.

Table 1 Rate constant of Jander's equation (k_j) and activation energy (E_a) of $FeVO_4$ formation.

	Mixture	M1	M2	M3	M4	M5
Temperature (℃)						
	525			1.3×10^{-3}		1.5×10^{-3}
	550		1.7×10^{-3}	4.3×10^{-3}		5.0×10^{-3}
$k_j(hr^{-1})$	575	2.4×10^{-4}	6.0×10^{-3}	1.2×10^{-2}	8.0×10^{-4}	1.3×10^{-2}
	600	1.3×10^{-3}	2.0×10^{-2}		2.5×10^{-3}	6.3×10^{-2}
	625	5.0×10^{-3}			7.6×10^{-3}	
E_a (kcal/mol)		86	70	62	70	66

V^{5+}, Fe^{3+} and O^{2-} (or O_2) in the product $FeVO_4$ layer. However, the details of the diffusion mechanism (one way diffusion, counter diffusion and effect of gaseous oxygen) is not known at present. Figure 2 shows $[1-(1-\alpha)^{1/3}]^2$ vs. t plot of five mixture (**M1-M5**). The rate constant, k_j, and activation energy, E_a are summarizd in Table 1. The order of k_j is

$$k_{jM5} \simeq k_{jM3} > k_{jM2} > k_{jM4} > k_{jM1} \quad (2)$$

This order of k_j will arise from following factors;

(1) Difference in diffusivity (D) of diffusing species in product layers,

(2) Difference in number of contact points (N) between V_2O_5 and Fe_2O_3 particles[6], and

(3) Difference in concentration gradient (ΔC) of diffusing species across the product layer.

These factors will be discussed below.

3. 2 Influence of $FeVO_4$ crystallite property on k_j

Table 2 shows interplanar spacing (d_{hkl}) and diffraction peak breadth (β_{hkl}) of five $FeVO_4$ formed from **M1**, **M2** and **M3** which contains **V1**, **V2** and **V3**, respectively. The value of d_{hkl} of each crystal planes are the same regardless of the difference in mixtures, reaction temperatures and α-values, whereas β_{hkl}-values are changing irregularly. According to

Table 2 Interplanar spacing (d_{hkl}/A) and peak breadth at half maxmum intensity (β_{hkl}/deg) of $FeVO_4$ formed from **M1**, **M2** and **M3**.

Mixture	Reaction temp. (℃)	Reaction time (hr)	Fractional conversion (α)	Crystal face (h k l)	d_{hkl}/A	β_{hkl}/deg
M1	600	5	0.22	0 1 $\bar{1}$	6.43	0.104
				0 1 1	5.34	0.105
				0 1 2	3.55	0.104
				0 2 $\bar{2}$	3.22	0.108
M2	600	0.5	0.30	0 1 $\bar{1}$	6.43	0.140
				0 1 1	5.43	0.141
				0 1 $\bar{2}$	3.55	0.140
				0 2 $\bar{2}$	3.22	0.146
M2	600	1	0.40	0 1 $\bar{1}$	6.43	0.108
				0 1 1	5.34	0.109
				0 1 2	3.55	0.112
				0 2 $\bar{2}$	3.22	0.112
M2	575	2	0.29	0 1 $\bar{1}$	6.43	0.138
				0 1 1	5.34	0.142
				0 1 2	3.55	0.153
				0 2 $\bar{2}$	3.22	0.158
M3	575	1	0.31	0 1 $\bar{1}$	6.43	0.127
				0 1 1	5.34	0.130
				0 1 2	3.55	0.143
				0 2 $\bar{2}$	3.22	0.147

Hall[7], β_{hkl}-values is represented by Eq. (3),

$$\beta_{hkl}\cos\theta/K\lambda = 1/L_{hkl} + \eta_{hkl}\sin\theta/K\lambda \qquad (3)$$

where L_{hkl} is the crystallite size, η_{hkl} the lattice strain, λ the wave length of X-ray, θ the Bragg's angle and K the shape factor (0.9). Figure 3 shows the plots of $\beta_{hkl}\cos\theta/K\lambda$ vs. $\sin\theta/K\lambda$ for $(01\bar{1})$, (011), (012) and $(02\bar{2})$ crystal planes of five $FeVO_4$ in Table 2. The lines **c** and **d** show almost the same slope. This indicate that $FeVO_4$ produced at 575℃ from **M2** and **M3** have the same η_{hkl}-value irrespective of the difference in V_2O_5 and reaction time.

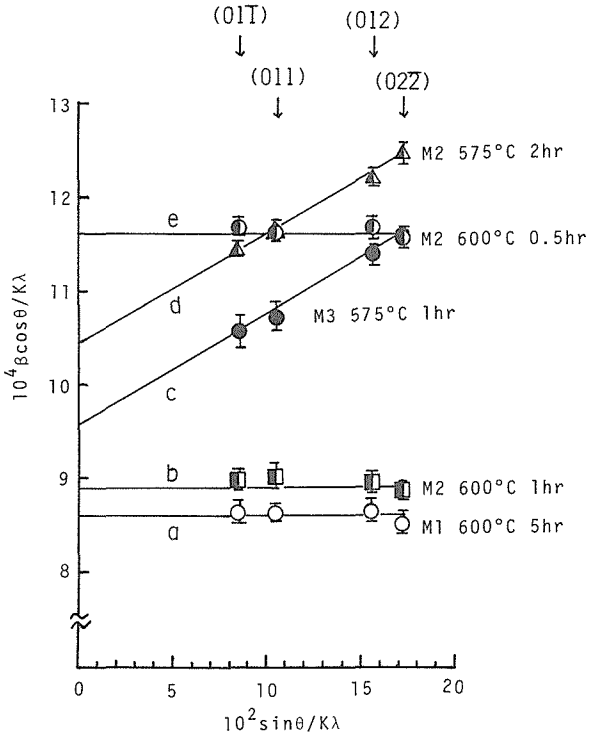

Fig. 3 Hall's plot of $FeVO_4$ formed under various conditions.

The horizontal lines of **a**, **b** and **e** show that $FeVO_4$ produced at 600℃ has no lattice strain. From these facts, it is suggested that $FeVO_4$ formed below 600℃ has a lattice strain, but not above 600℃ and that the strain depends on the reaction temperature alone, but is not dependent on the difference in V_2O_5 samples. The intercept of five lines indicates an increase in L_{hkl}-value with reaction temperature and time. Consequently, the strain of $FeVO_4$ layer formed in **M1**-**M5** will have the same value at the same reaction terperature. Furthermore, $FeVO_4$ has the same d_{hkl}-value as shown in Table 2. These facts suggest that the diffusivity in the product layer is equal to the five mixtures and hence has only has a minor effect on the change of k_j in Eq. (2).

3. 3. Infiluence of particle size on k_j

Figure 4 shows SEM photographs of V_2O_5 (**V1**-**V3**) and Fe_2O_3 (**F1** and **F2**) before mixing. Fig. 4-(A) and (D) indicate that **V1** and **F1** consist of particles larger than 3 μm

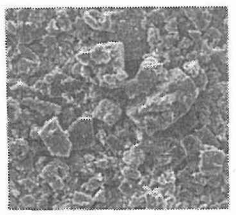

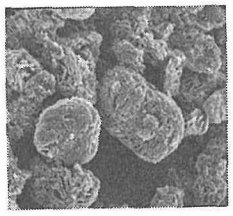

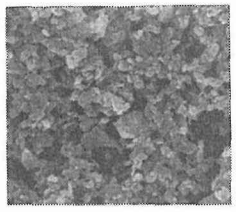

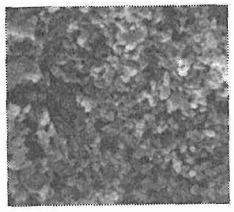

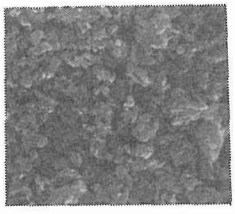

Fig. 4 SEM photographs of V_2O_5 (**V1**-**V3**) and Fe_2O_3 (**F1**, **F2**) samples.

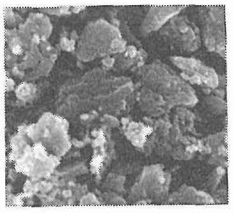

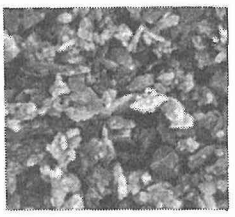

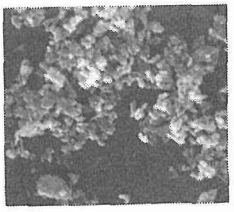

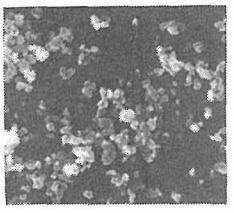

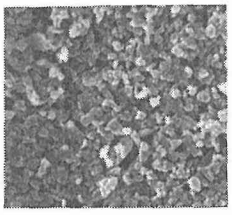

Fig. 5 SEM photographs of V_2O_5 and Fe_2O_3 mixtures (**M1**-**M5**). Symbols in brackets show the kind of V_2O_5 and Fe_2O_3 samples and mixing force (strong and weak force).

and 10 μm, respectively. On the other hand, the particle sizes of **V2**, **V3** and **F2** (Figs. 4-(B), (C) and (E)) are found to be in a range of 0.2-1.0 μm. The average particle size of these samples was 0.4 μm. Then the order of the particle sizes of samples before mixing can be estimated to be **V1**$>$**V2**$\simeq$**V3**$\simeq$**F2** and **F1**$>$**F2**.

Figure 5 shows SEM photographs of the mixtures (**M1**-**M5**). The particle sizes of **M2**, **M3** and **M5** are observed to be almost the same. Their average particle size was 0.4 μm. The particle sizes of **M1** and **M4** were setimated to be 0.9 μm and 0.7 μm, respectively.

From a comparison of the average sizes described above, it can be seen that the mixing process results in the reduction of the particle size of **V1** and **F1** to some extent and the order of particle sizes of V_2O_5 and Fe_2O_3 in the mixtures **M1**-**M5** is

$$d_{V1(in\ M1)} > d_{V2(in\ M2,\ M4\ and\ M5)} \simeq d_{V3(in\ M3)} \simeq d_{F2(in\ M1,\ M2,\ M3\ and\ M5)}$$
$$and\ \ d_{F1(in\ M4)} > d_{F2(in\ M1,\ M2,\ M3\ and\ M5)} \qquad (4)$$

Since the distinction of V_2O_5 from Fe_2O_3 particles in SEM photographs of the mixtures was not possible, the particle size distribution of model particles of V_2O_5 was measured to test the order in Eq. (4). The model V_2O_5 particles in **M2**, **M3** and **M5** were prepared by grinding **V2** with a weak force for 1 hr, **V3** with weak force for 1 hr and **V2** with a strong force for

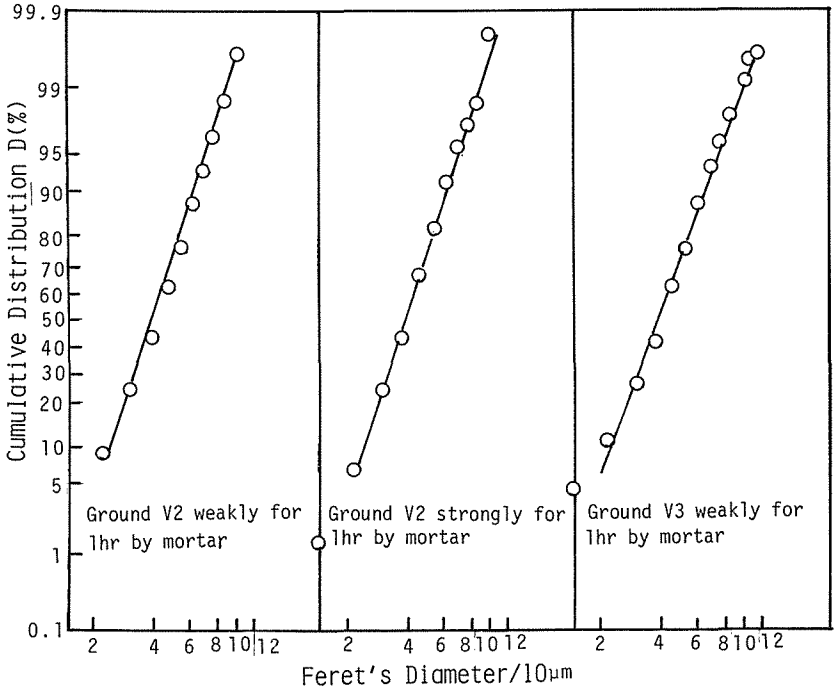

Fig. 6 Particle size distribution of model V_2O_5 powders.

1 hr, respectively. Figure 6 shows particle size distribution. Feret's diameter[8] was measured on more than one thousand of V_2O_5 particles. The three lines showing logarithmic normal distribution have the same slope and the same median diameter ($D_{50\%}=0.4\,\mu m$). The $D_{50\%}$-value agrees with the particle size estimated from SEM photographs in Figs. 4-(B), (C), (E), 5-(B), (C) and (E).

As pointed out by Komatsu[6], the rate of powder reaction depends on the number of contact points (contact area) between the reacting particles and the number increases with the decrease in the particle sizes. Then, the order of reaction rate for **M1**-**M5** is expected to be

$$\mathbf{M5} \simeq \mathbf{M3} \simeq \mathbf{M2} > \mathbf{M4} > \mathbf{M1} \qquad (5)$$

on the basis of Eq. (4), provided that the particle shape effect on the number can be ignored. This order partly agrees with the order of k_j in Eq. (2). Accordingly, k_j is suggested to depend upon not only the contact points but also other factors.

3. 4 Effect of grinding on X-ray diffraction peak breadth at half maximum intensity (β_{hkl}), specific surface area (S) and infrared spectra of the samples.

Table 3 shows β_{hkl} and S for V_2O_5 (**V1**, **V2**, **V3** and **V2'**) and Fe_2O_3 (**F1** and **F2**) samples before the mixing, and the frequency of IR spectrum of the stretching vibration of V=O (ν). Sample **V2'** was prepared as model particles of V_2O_5 for **M5** described in section **3. 3**, which was obtained by grinding **V2** with a strong force for 1 hr. β_{hkl} of **V2** and **V3** are larger than those of **V1** and β_{hkl} of **V2'** are slightly larger than those of **V2**, which indicate that β_{hkl} increases by strong force grinding and jet-mill-grinding. However, it was obser-

ved that β_{hkl} of **V2** was not increased by a weak force grinding for 1 hr and β_{hkl} of Fe_2O_3 (**F1** and **F2**) was not changed by grinding even with a strong force. The mixtures of **M1**, **M2**, **M3** and **M4** were prepared by appling a weak mixing force, then the order of β_{hkl}-value of V_2O_5 in the mixtures will be **M3(V3)** > **M2(V2)** = **M4(V2)** > **M1(V1)**. This order coincides with the order of k_j (Eq. (2)) except for **M5** and hence suggests that the rate is affected by the crystallite properties of V_2O_5.

Table 3 X-ray diffraction peak breadth at half-maximum intensity (β_{hkl}), specific surface area (S) and stretching vibration frequency (ν) of samples.

Sample	V_2O_5				Fe_2O_3	
	V1	**V2**	**V2′**	**V3**	**F1**	**F2**
β_{hkl}/heg						
β_{600}	0.077	0.086	0.090	0.106		
β_{400}	0.060	0.064	0.069	0.091		
β_{200}	0.044	0.049	0.050	0.060		
β_{110}					0.075	0.075
β_{104}					0.096	0.096
S/m^2g^{-1}	7.3	7.1	7.4	8.9	5.2	5.3
ν/cm^{-1} (V=O bond)	1022	1021	1021	1017		

V2′: Ground **V2** for 1 hr by hand with strong force in mortar.

The surfcce area (S) of **V3** is slightly larger than that of **V1**, **V2** and **V2′**, which indicates that S-value is increased by jet-mill-grinding, however it remained unchanged in the case of mortar grinding. No remarkable effect of grinding is seen in IR frequency (ν) for four V_2O_5.

3. 5 Influence of lattice strain of V_2O_5 samples on k_j

Figure 7 shows Hall's plot of **V1**, **V2**, **V2′** and **V3** on the basis of β_{hkl} (hkl=200, 400, 600) in Table 3. L_{hkl} and η_{hkl}-values in Eq. (3) derived from three (h00) planes are represented by L_a and η_a-values, respectively. η_a-value corresponds to the distribution of interplanar spacing ($<\Delta d/d>$) in V_2O_5 crystal, which arises from the displacement of V_2O_5 lattice from the normal position along a-axis. Then η_a-value may be a parameter showing the disorder of V_2O_5 crystal. In Fig. 7, **V1**, **V2** and **V2′** show the straight lines giving the same intercept, which corresponds to the same L_a-values of these V_2O_5. The L_a-value was estimated to be about 2500A which coincides with equivalent specific surface diameter, D_s, calculated from $6\times10^4/d_s\cdot S$ where d_s is density of V_2O_5 (3.4 g/cm³) and S is the specific surface area of **V1**, **V2** and **V2′** in Table 3, by assuming that the crystallites are spherical or cubic. The slope of the line for **V1**, **V2** and **V2′** indicates that the

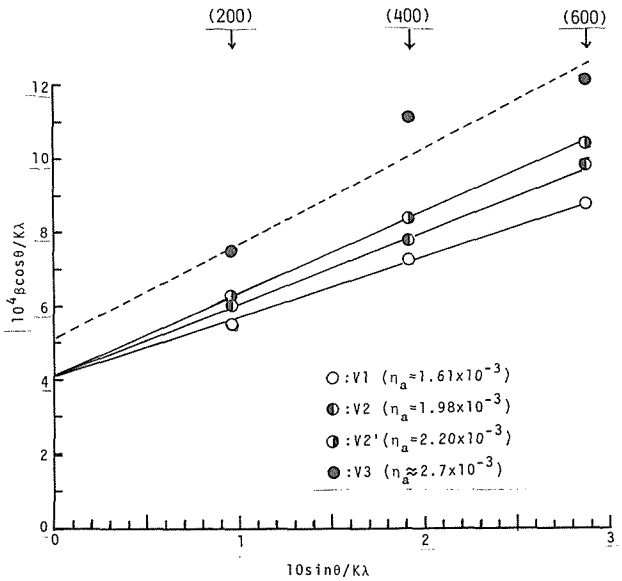

Fig. 7 Hall's plot of V_2O_5 samples.

grinding results in an increases of the lattice strain of V_2O_5 crystallite in tha order of **V1**< **V2**<**V2'**.

In order to discuss the reason for lesser linearity of **V3** in Fig. 7, 2θ of **V1**, **V2** and **V3** of (200), (400) and (600) planes were compared with those of the standard V_2O_5 ($\mathbf{V_s}$) (Table 4). The deviation in 2θ of each crystal plane from those of $\mathbf{V_s}$ increases in the order of **V3**>**V2**>**V1**. According to Nelson *et. al*[9]. in the case of a perfect crystal, the product of interplanar spacing (d_{h00}) and Miller index (h) should change linearly with Nelson -Riley's function, $1/2(\cos^2\theta/\theta+\cos^2\theta/\sin\theta)$ where θ is the Bragg's angle. Figure 8 shows the Nelson-Riley's plot of the data in Table 4. Three points of $\mathbf{V_s}$ (≦) show a single straight line. This means that in the case of $\mathbf{V_s}$, three 2θ-values provide the single cell constant (11.484A). On the other hand, the points of **V1**, **V2** and **V3** deviate from the line of $\mathbf{V_s}$. These deviations are assumd to be due to the stacking fault of V_2O_5 as in the case of Cu-Si alloy shown by Otte[10]. Thus **V3**, showing the largest deviation in Fig. 8, is affected most extensively by the stacking fault. The less-linearity of **V3** in Fig. 7, is considered to be attributed to the stacking fault. η_a-value of **V3** was roughly estimated in the following manner in Fig. 7. Since L_a is approximately equal to D_s calculated by S-value, $1/L_a$-value of **V3** was calculated by S. The dotted line in Fig. 7 was ruled by the least-square method. **V3** shows the largest η_a-value. From these results, the order of the lattice strain of V_2O_5 in **M1**-**M5** is assumed to be Eq. (6).

$$\eta_{aM3} > \eta_{aM5} > \eta_{aM2} > \eta_{aM4} > \eta_{aM1} \qquad (6)$$

Eq. (6) partly agrees with the order of k_j (Eq. (2)). Thus k_j-value is suggested to be dependent upon η_a-value of V_2O_5.

In the reaction of V_2O_5 with Fe_2O_3, V_2O_5 may be one of the diffusing components. Thus Eq. (6) suggests that η_a relates to the concentration gradient (ΔC) of V^{5+} across the product layer. As mentioned in section **3. 1**, k_j is

Table 4 X-ray diffraction angle ($2\theta/deg$) of V_2O_5 ($\mathbf{V_s}$, **V1**, **V2** and **V3**).

	$2\theta/deg$ (Crkα)		
Crystal plane	(2 0 0)	(4 0 0)	(6 0 0)
$\mathbf{V_s}$ (annealing **V2**)	22.811±0.002	46.841±0.001	73.360±0.001
V1	22.811±0.002	46.847±0.001	73.361±0.001
V2	22.812±0.002	46.850±0.001	73.350±0.001
V3	22.816±0.002	46.852±0.001	73.330±0.001

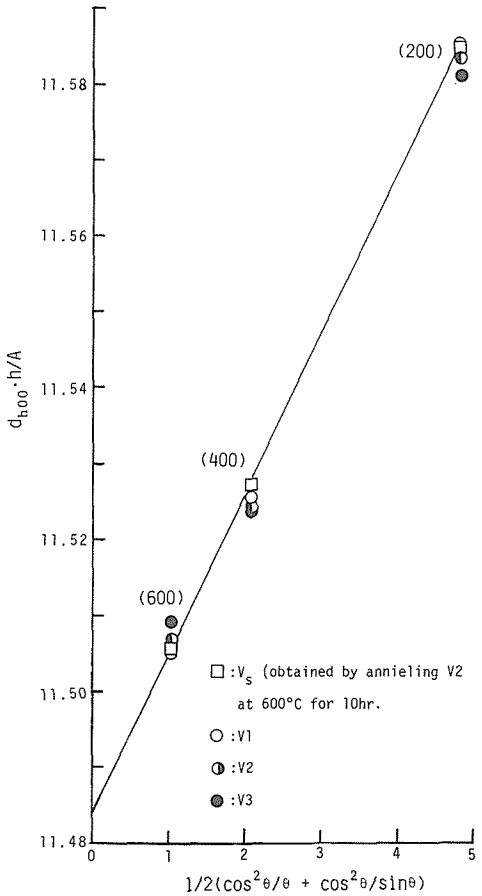

Fig. 8 Nelson-Riley's plot of V_2O_5 samples.

determined by D, N and ΔC. D was assumed to have a minor effect on the difference of k_j in Eq. (2). The effect of N and ΔC was shown by Eqs. (5) and (6). From these two equations the expected order of k_j will be

$$\mathbf{M3} \gtrsim \mathbf{M5} \gtrsim \mathbf{M2} \gtrsim \mathbf{M4} > \mathbf{M1} \tag{7}$$

This order agrees with Eq. (2), except for **M5**. **M5** was prepared with a strong mixing force and **M3** was prepared with a weak force. A possible explanation may be that a larger contact area of **M5** than **M3** due to the strong mixing force leads to a similar k_j.

Reference

1) A. Shimizu, R. Furuichi and T. Ishii, J. Chem. Soc. Jap. Chemistry and Industrial Chemistry, 39 (1975).
2) A. Shimizu, R. Furuichi and T. Ishii, Bull. Faculty of Eng. Hokkaido Univ., **78,** 77 (1976).
3) S. F. Bartram, "Hand Book of X-rays", MaGraw-Hill (1967) 17-9.
4) J. H. Sharp, G. W. Brindley and B. N. Narahari Achar, J. Am. Cer. Soc., **49,** 7, 379 (1966).
5) W. Jander, Z. Anorg. Alleg. Chem., **163,** 1 (1927).
6) W. Komatsu and T. Uemura, Z. Phys. Chem., Neue Folge, **72,** 59 (1970).
7) W. H. Hall, Proc. Phys. Soc., A, **62,** 741 (1949).
8) T. Allen, "Particle Size Measurement" Chapman and Hall, London (1968).
9) J. B. Nelson and D. P. Riley, Proc. Phys. Soc., **57,** 160 (1945).
10) H. M. Otte, J. Appl. Phys., **33,** 1436 (1962).